An Understanding of the Electrophilic/Nucleophilic Behavior of Electro-Deficient 2,3-Disubstituted 1,3-Butadienes in Polar Diels−Alder Reactions. A Density Functional Theory Study

Luis R. Domingo,*,† Eduardo Chamorro,‡ and Patricia Pérez‡

Departamento de Química Orgánica, Universidad de Valencia, Dr. Moliner 50, E-46100 Burjassot, Valencia, Spain, and Departamento de Ciencias Químicas, Laboratorio de Química Teórica, Facultad de Ecología y Recursos Naturales, Universidad Andrés Bello, Av. República 275, 837-0146 Santiago, Chile

Received: December 13, 2007; In Final Form: February 14, 2008

The electrophilic/nucleophilic behavior of dimethyl 2,3-dimethylenesuccinate **1**, an electron-deficient 2,3-disubstituted 1,3-butadiene, in polar Diels−Alder reactions has been studied using DFT methods at the B3LYP/6-31G(d) level of theory. The electronic nature of bonding of the transition structures involved in the cycloaddition reactions of the diene **1** toward the nucleophilically activated dienophile **6** and the strong electrophilically activated dienophile **7** has been carefully examined within the natural bond orbital (NBO) and the topological analysis of the electron localization function (ELF) frameworks. Additionally, a study of the global electrophilicity pattern of the reagents at the ground state was performed. This evidence allows us to rationalize the participation of electron-deficient 2-susbtituted and 2,3-disubstituted 1,3-butadienes as nucleophiles in polar Diels−Alder reactions.

Introduction

The Diels−Alder (DA) reaction is arguably one of the most powerful reactions in the arsenal of the synthetic organic chemist.[1] By varying the nature of the diene and dienophile, many different types of carbocyclic structures can be built up. However, not all possibilities take place easily. For instance, the DA reaction between butadiene and ethylene must be forced to take place: after 17 h at 165 °C and 900 atm, it does give a yield of 78%.[2] However, the presence of electron-withdrawing substituents in the dienophile and electron-releasing substituents in the diene or vice versa can drastically accelerate the process.[3]

For a long time, Domingo's group has been interested in the study of the molecular mechanism of the polar DA reactions.[4] These studies point out a relationship between the decrease of the activation barrier of the cycloaddition and the charge transfer (CT) along a nonsynchronous bond-formation process. Thus, the increase of the electron-rich character of the diene (the nucleophilicity) together with the increase of the electron-poor character of the ethylene derivative (the electrophilicity) or vice versa results in an enhancement in the CT, which is accompanied by the drop of the activation barrier.[4a,b]

We have reported the use of the global electrophilicity index, ω, proposed by Parr et al.[5] to classify the global electrophilicity of a series of dienes and dienophiles currently present in DA reactions.[6] We found a good linear correlation between the difference in electrophilicity for the diene and dienophile pair, $\Delta\omega$, and the polar character of a DA reaction.[6]

Spino et al.[7] reported an experimental study of the DA reactions of dimethyl 2,3-dimethylenesuccinate **1**, an electron-deficient (ED) diene, with a wide variety of electron-rich (ER) ethylenes, including the 1,1-diethoxyethene **2** (R = Et) and ethyl vinyl ether **3** (R = Et), and ED ethylenes, including methyl acrylate **4** (R = Me) and diethyl 2-methylenemalonate **5** (R = Et) (see Scheme 1). Some observations were drawn from the kinetic results: (i) the faster DA reaction corresponds to the cycloaddition between the ED diene **1** and the ER ethylene **2** (R = Et); (ii) the k_r for cycloaddition between the ED diene **1** and the ER ethylene **2**, 0.77 mL mol^{-1} s^{-1}, is only twice larger than that for the reaction between ED diene **1** and the ED ethylene **5** (R = Et), 0.26 mL mol^{-1} s^{-1}; and (iii) the cycloadditions involving the disubstituted ethylenes **2** and **5** are faster than those involving the monosubtituted ones **3** and **4**.

The frontier molecular orbital (FMO) theory[8] was used by these authors to predict the reactivity of these reagents in DA reactions.[7] Spino et al. concluded that, in the normal electron demand (NED) DA reaction, the FMO theory could predict the relative reactivity, while in the case of the inverse electron demand (IED) one, it could not.[7] In this work, several questions were raised, but they were not resolved: Why do a series of 2-azadienes react with a host of ED ethylenes including methyl acrylate, but none react with ER vinyl ether?[9] Why does 2-carbometoxy-1,3-butadiene dimerize much faster than it reacts with ER reagents?[10] Note that these cases are similar to the DA reaction between the ED diene **1** and the ED ethylene **5**, which has a rate of the same order of magnitude as that for the reaction between the ED diene **1** and the ER ethylene **2**. In these cases, the choice of which pair of frontier orbitals takes place is sometimes difficult because of the closer HOMO−LUMO gap energies for both ED reagents.

More recently, Domingo[4c] presented a density functional theory (DFT) analysis for a short series of DA reactions between the ED diene **1** and the ER ethylenes **2** (R = Me) and **3** (R = Me) and the ED ethylenes **4** and **5** (R = Me) as models of these DA reactions studied by Spino et al. (see Scheme 1). Both the natural bond orbital (NBO) analysis of electronic structure of the transition structures (TSs) involved in these DA reactions and the study of the global and local reactivity index at the ground state (GS) of the reagents allowed us to explain the

* Corresponding author.
† Universidad de Valencia.
‡ Universidad Andrés Bello.

10.1021/jp711704m CCC: $40.75
Published on Web 03/28/2008

SCHEME 1

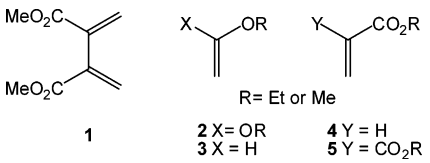

SCHEME 2

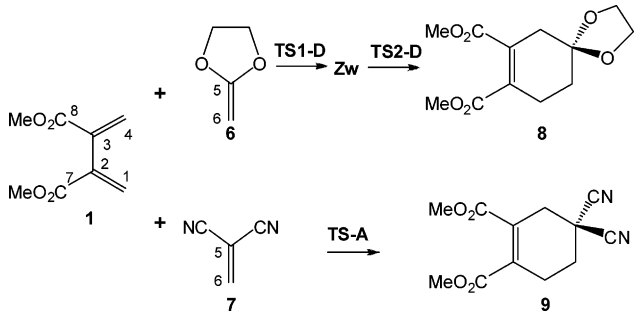

participation of the ED diene **1** as nucleophile in a polar DA reaction toward strong electrophiles as **5**.

Now, we present a theoretical analysis on the electronic structure of the TSs involved in the DA reactions of the ED 2,3-disubstituted 1,3-butadiene **1** toward the nucleophilically activated dienophile **6**, 2-methylene-1,3-dioxolane, and a strong electrophilically activated dienophile **7**, 1,1-dicyanoethylene. The purpose of this study is the characterization of the dual electrophilic/nucleophilic behavior of the ED butadiene **1** (see Scheme 2). We want to give an explanation for the participation of these ED 2,3-disubstituted 1,3-butadienes as nucleophiles in polar DA reactions toward strong electrophilically activated ethylenes. This reactivity, which it is not easily explained using the FMO model, can be predicted by an analysis of the reactivity indexes defined within the conceptual DFT.[11]

Computational and Theoretical Methods

DFT calculations were carried out using the B3LYP[12] exchange-correlation functionals, together with the standard 6-31G(d) basis set.[13] This level of theory has been shown suitable to provide enough good performance in the analysis of both geometric and electronic properties in the DA reactions.[11b] The optimizations were carried out using the Berny analytical gradient optimization method.[14] The stationary points were characterized by frequency calculations in order to verify that the TSs have one and only one imaginary frequency. The intrinsic reaction coordinate (IRC)[15] path was traced in order to check the energy profiles connecting each TS to the two associated minima of the proposed mechanism by using the second-order González−Schlegel integration method.[16] The electronic structures of stationary points were analyzed by the NBO method[17] and the topological analysis of the electron localization function (ELF).[18] The electron localization function $\eta(r)$[18,19] constitutes a measure of the spin pair distribution. It allows us to identify those regions where the relative probability of finding electrons with parallel spin close together is high (i.e., where the local Pauli repulsion is strong and conveniently $\eta(\mathbf{r}) \rightarrow 0$) from those with a high probability of finding a single electron or a pair of opposite spin electrons (i.e., $\eta(\mathbf{r}) \rightarrow 1$). This analysis has been recently generalized also to the analysis of correlated wavefunctions.[19h] The topological analysis of $\eta(\mathbf{r})$ (e.g., the analysis of the gradient field of $\eta(\mathbf{r})$)[19c−f] provides a partition of the molecular space into non-overlapping volumes (e.g., basins) that can be associated with entities of chemical significance as atomic cores and valence regions (e.g., bonds or lone pairs). Valence basins are indeed clasified in terms of the number of core basins with which they share a boundary (e.g., the synaptic order).[19c] This has been found a useful tool to rationalize the electron delocalization in molecular systems.[19c,f,g,20−22] The topological analysis of ELF been probed to be a useful tool to give a deeper insight into the nature of the chemical bonding in a variety of stationary and reacting systems,[20−22] including for instance, the analysis of pericyclic processes,[20a−g] cycloaddition reactions,[22] radical systems,[20i] and aromaticity.[20j,k] The integration of the one- and two-electron density probabilities in these basins provides indeed a powerful quantitative population analysis. The average basin population in the basin i is the result of integrating the electron density $\rho(\mathbf{r})$ in such domain, $N_i = \int_i \rho(\mathbf{r})\, d\mathbf{r}$. The variance σ_i^2 (e.g., the square of the standard deviation or quantum uncertainty) of the population basin can be written in terms of contributions of the remaining basins, $\sigma_i^2 = \sum_{j\neq i} B_{ij}$, where $B_{ij} = N_i N_j - N_{ij} = -\int_i \int_j d\mathbf{r}_1 d\mathbf{r}_2 \rho(\mathbf{r}_1)\rho(\mathbf{r}_2)h(\mathbf{r}_1, \mathbf{r}_2)$ are written in terms of the basin populations N_i and the exchange-correlation hole $h(\mathbf{r}_1, \mathbf{r}_2)$. Note that the variance measure the net "excess" of electron pairs that are formed within a given basin in comparison to the classical number that could be expected from the average number of electrons localized there. Thus, covariances constitute useful advice helping to rationalize the pattern of electron delocalization in molecular systems. Note that σ_i^2 could be associated with the amount of the electron population of basin i considered as fluctuating, while the terms B_{ij} correspond to the contributions to such fluctuation arising from the basin j (i.e., coming from the delocalization of the exchange correlation hole on the basin j). Our analyses of delocalization have been performed within such framework by using relative cross fluctuation terms as $r_{ij} = B_{ij}/N_i$ or, equivalently, as fluctuation contributions expressed in percentage, $p_{ij} = (r_{ij}/\lambda_i) \times 100$, where the localization index, λ_i, corresponds simply to $\lambda_i = \sum_{j\neq i}(r_{ij}) = \sigma_i^2/N_i$. The fluctuation contributions p_{ij} has been included as Supporting Information in the last column of Tables S.I and S.II and are interpreted here as the contribution of delocalization of population in basin j to the variance of the population in the basin i, $\overline{N_i}$; $p_{ij} = (B_{ij}/\sigma_i^2) \times 100$. These interpretations are of course arbitary by definition and are used in the present context as an ansatz. The ELF study was performed with the TopMod program[23] using the corresponding monodeterminantal wave functions for transition state structures. All calculations were carried out using the Gaussian03 suite of programs.[24]

The global electrophilicity index,[5] ω, which measures the stabilization energy when the system acquires an additional electronic charge ΔN from a perfect donor environment, is given by the following simple expression, $\omega = \mu^2/(2\eta)$, in terms of the electronic chemical potential μ and the chemical hardness η.[5,25] Both quantities may be approached in terms of the one electron energies of the frontier molecular orbital HOMO and LUMO, ϵ_H and ϵ_L, as $\mu \approx (\epsilon_H + \epsilon_L)/2$ and $\eta \approx (\epsilon_L - \epsilon_H)$, respectively.[11a,26]

Results and Discussions

First, the energies and geometries of the stationary points found in the potential energy surfaces (PES) for the two cycloadditions will be discussed. Then, the results from the NBO and ELF analysis of the electronic structure of the TSs involved in these reactions are discussed in order to establish the nature of the electronic rearrangement in these cycloadditions. The polar character of these DA reactions will be finally analyzed

TABLE 1: Total (*E*, in au) and Relative[a] (Δ*E*, in kcal mol^{-1}) Energies of the Stationary Points Involved in the Diels−Alder Reaction between the Diene 1 and the ER Ethylene 6, and the ED Ethylene 7

	E	Δ*E*
1	−611.737824	
6	−306.441320	
TS1-D	−918.158987	12.6
Zw	−918.160381	11.8
TS2-D	−918.160362	11.8
8	−918.232455	−33.5
7	−263.062684	
TS-A	−874.775637	15.6
9	−874.851206	−31.8

[a] Relative to **1** + **6** or **1** + **7**.

on the basis of the electrophilicity index defined within the conceptual DFT.

1. Energies. Analysis of the stationary points associated to the formation of the cycloadducts **8** and **9** indicates that both DA reactions present different molecular mechanisms. While the reaction between the ED diene **1** and the ER ethylene **6** presents a two-step mechanism via the formation of a zwitterionic intermediate, the reaction of the ED diene **1** with the ED ethylene **7** presents an one-step mechanism through a highly asynchronous TS (see Scheme 2). Therefore, two TSs, **TS1-D** and **TS2-D**, and a zwitterionic intermediate, **Zw**, associated with the two-step reaction of the ED diene **1** with the ER ethylene **6**, one **TS-A** associated to the one-step reaction of the ED diene **1** with the ED ethylene **7**, and the corresponding cycloadducts **8** and **9**, were located and characterized.

The activation energies associated to the DA reactions of the ED diene **1** with the ER ethylene **6**, and with the ED ethylene **7** are 12.6 (**TS1-D**) and 15.6 (**TS-A**) kcal·mol^{-1}, respectively (see Table 1). These values are slightly lower than those obtained for the reaction of the diene **1** with ER ethylene **2**, 15.3 kcal·mol^{-1}, and with the ED ethylene **5**, 16.3 kcal·mol^{-1},[4c] as a consequence of the slightly larger nucleophilic character of **6** than **2** and the larger electrophilic character of **7** than **5** (see later). The activation energy for the DA reaction between the ED diene **1** and the ED ethylene **7** is only 3 kcal·mol^{-1} higher than that for the reaction between the ED diene **1** and the ER ethylene **6**, but approximately 10 kcal·mol^{-1} lower than the activation energy for the DA reaction between 1,3-butadiene and ethylene.[27] These energy results point out that not only the presence of electron-withdrawing substituents on ethylene and electron-releasing substituents on the butadiene, or vice versa, activates the DA reaction through a polar process, but also the reactions between reagents possessing electron-withdrawing substituents (see later). Note that the presence of only electron-releasing substituents on both reagents does not favor the DA reaction.[28] At the stepwise mechanism, the zwitterionic intermediate **Zw** is located 11.8 kcal·mol^{-1} above the separated reagents. The intermediate **Zw** with an unappreciable barrier is converted in the corresponding cycloadduct **8**. Finally, the formation of the **8** and **9** cycloadducts is strongly exothermic in −33.5 and −31.8 kcal·mol^{-1}, respectively.

2. Geometries. The geometries of the TSs are given in Figure 1. The lengths of the C1−C6 and C4−C5 forming bonds at the TSs are 1.921 and 3.561 Å at **TS1-D** and 1.964 and 2.866 Å at **TS-A**, respectively. In both TSs, the long-distance between the C4 and the C5 atoms indicates that any covalent interaction exists between these terminal atoms. These data for **TS-A** indicate that it corresponds to a highly asynchronous bond-formation process. The IRC from **TS-A** to the cycloadduct **9** indicates that the cycloaddition takes place via a one-step two-stage mechanism.[29] At the first stage of the reaction, only the C1−C6 σ bond is being formed. On going from **TS-A** to **9**, the reaction progresses with the formation of the C1−C6 bond and, only when it is formed, begins the formation of the C4−C5. On the other hand, in the reaction of **1** with **6**, the **TS1-D** yields first to the intermediate **Zw** at which the length of the C1−C6 bond is 1.690 Å, while the distance between the C4 and the C5 atoms is 3.390 Å. Finally, at **TS2-D**, the length of the C4−C5 forming bond becomes 3.106 Å.

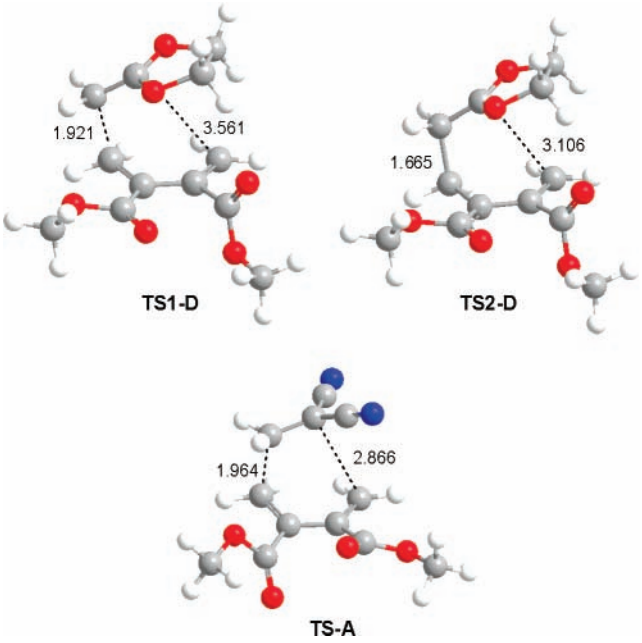

Figure 1. Transition structures involved in the stepwise Diels−Alder reaction between the diene **1** and the ER ethylene **6**, **TS1-D** and **TS2-D**, and in the one-step Diels−Alder reaction of **1** with the ED ethylene **7**, **TS-A**. The distances are given in angstroms.

It is worth noting some relevant geometrical parameter of the butadiene fragment at the TSs associated to the C1−C6 bond formation. The lengths of the C2−C3 and C2−C7 (COOMe) bonds at the TSs are 1.452 and 1.452 Å at **TS1-D** and 1.433 and 1.500 Å at **TS-A**, while these lengths at the diene **1** are 1.487 and 1.495 Å, respectively. Thus, while for the reaction of the diene **1** with the ER ethylene **6**, the C2−C7 bond undergoes a length shortening; for the reaction of the diene **1** with the ED ethylene **7**, the length shortening corresponds to the diene C2−C3 (C═C) bond. On the other hand, while at the **TS1-D**, the COOMe group located at the C2 position of the diene **1** is coplanar to the diene system, the COOMe group at the C3 position is twisted (see Figure 1). A different behavior is found at **TS-A** where the COOMe group present at the C2 position of **1** is now twisted.

These geometrical parameters point out a different participation of the COOMe group present on the C2 position and the C3−C4 double bond of the butadiene system of **1** along the two cycloadditions. While at the DA reaction of the diene **1** with the ER ethylene **6** the COOMe group located on the C2 conjugated position participates on the first stage of the reaction acting as an electron-withdrawing group, at the DA reaction of the diene **1** with the ED ethylene **7** is the C3−C4 double bond that participates as a electron-releasing susbtituent, shortening the C2−C3 length and twisting the COOMe group located at the C2 position.

3. Analysis of the Electronic Structure of TS1-D and TS-A. The electronic structure of these cycloadditions was analyzed by using the Wiberg bond order (BO)[30] and the natural charges

obtained by a NBO analysis.[17] The electronic structure analysis is complemented through an ELF analysis of the TSs that are involved in the first stage of these cycloadditions, namely, **TS1-D** and **TS-A**.

3.1. NBO Analysis. The BO values between the C1 and C6 and the C4 and C5 atoms at the TSs are 0.56 and 0.05 at **TS1-D** and 0.51 and 0.14 at **TS-A**, respectively. These data point out the high asynchronicity on the bond formation. At these TSs, the larger bond formation corresponds to the two-center interaction between the end of the butadiene system of **1**, the C1 carbon, and the β-conjugated positions of the substituted ethylenes **6** and **7**, the C6 carbon atom. The more favorable **TS1-D** is slightly more advanced and more asynchronous than the **TS-A**.

The BO values of the C1−C2, C2−C3, C3−C4, and C2−C7 bonds at these TSs are 1.31, 1.15, 1.73, and 1.13 at **TS1-D** and 1.39, 1.21, 1.64, and 0.98 at **TS-A**. The BO values of the C2−C3 (C═C) and C2−C7 (COOMe) bonds at these TSs show the different behavior of the butadiene system and the C2 conjugated COOMe group at these polar DA reactions. Thus, at the DA reaction between the ED diene **1** and the ER ethylene **6**, both geometrical parameter and BO values point out the participation of the COOMe group located on C2, which acts as an electron-withdrawing group. However, along the attack of the diene **1** to the ED ethylene **7**, these data point out the participation of the C3−C4 double bond of 1,3-butadiene, which acts as an electron-releasing group through its π system. This behavior is shown through the decrease of the BO value of the C3−C4 double bond and the increase of the BO value of the C2−C3 single bond as a consequence of the delocalization of the electron density of the C3−C4 π system on the C2 carbon atom. Finally, at both TSs, the BO value of the C3−C8 single bond, 0.95 at **TS1-D** and 0.98 **TS-A**, indicates an unappreciable participation of the COOMe group located on C3 on both cycloadditions (see later). Note that the substitution on the C3 position does not corresponds to any conjugate position relative to the C1 carbon.

The natural population analysis (NPA) allows the evaluation of the CT and its direction at these polar DA reactions. The B3LYP/6-31G(d) natural atomic charges at the TSs associated to the two-center interactions were shared between the diene **1** and the substituted ethylenes **6** and **7**. The net charge at the butadiene fragment at these TSs is predicted to be −0.41e at **TS1-D** and +0.20 e at **TS-A**. Some relevant conclusions can be redrawn from these values: (i) first, these values indicate that these TSs have some zwitterionic nature corresponding to polar processes; (ii) the more favorable **TS1-D** presents the larger CT as a consequence of the favorable interactions between the ends of the electrophilically activated ED diene **1** and the nucleophilically activated ER ethylene **6**; (iii) there is a change of the direction of the electron density transfer at both TSs. While at **TS1-D**, the CT flows from the ER ethylene **6** to the ED diene **1**; at **TS-A**, there is a change on the direction; now the CT goes from the diene **1** toward the strong electrophilically activated ED ethylene **7**. Finally, (iv) these CTs are slightly larger than those obtained for the DA reaction between the diene **1** and the ethylenes **2** and **5** as a consequence of the more nucleophilic and electrophilic character of the ethylenes **6** and **7** than the ethylenes **2** and **5**, respectively (see later). These results corroborate the observed finding in polar DA reactions that the increase of the CT at the TSs goes accompanied with a drop of the activation energy associated with these polar DA reactions.[4a,b,6]

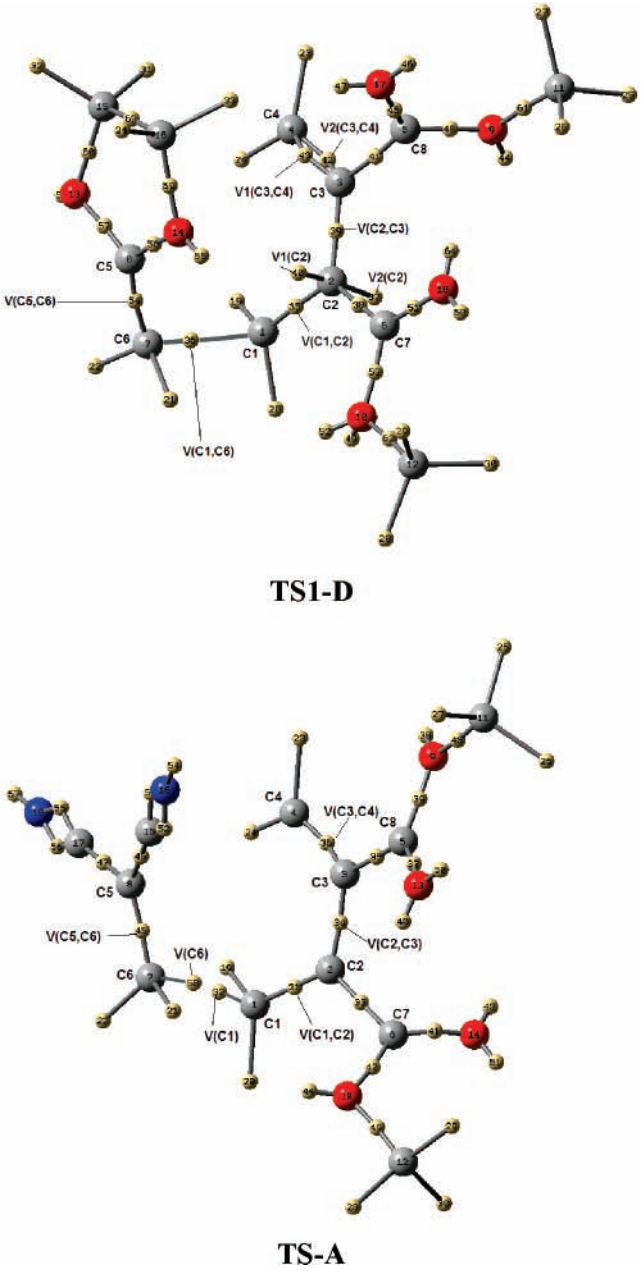

Figure 2. Spatial localization of the maxima (e.g., attractors) of the electron localization function (ELF) for **TS1-D** and **TS-A**.

3.2. ELF Topological Analysis. Understanding that the technical details and nomenclature of this methodology are widely available,[18−22] we focus directly on its application to the rationalization of electron delocalization associated with **TS-A** and **TS1-D** transition structures in order to further characterize the electronic nature of these polar cycloadditions. There exists ELF maxima (e.g., attractors) located in the region associate to the C1−C6 bond forming in both TSs, whereas no evidence for attractors associated with the C4−C5 bond region can be found for these two highly asynchronous TSs. In the case of **TS1-D**, the associated basin is indeed disynaptic, **V(C1,C6)**, localizing 1.02e (see Figure 2 and Table SI.I in Supporting Information). In **TS-A**, two monosynaptic basins each associated with the carbon interacting centers can be identified: **V(C1)** and **V(C6)**, which have populations of 0.46e and 0.25e, respectively (see Table SI.II in Supporting Information). The variances for these population are 0.73, 0.46, and 0.23, respectively, giving high delocalization values in such regions corresponding to ∼72% for **V(C1,C6)** in the case of

TS1-D and to ∼86%, and ∼91% for **V(C1)** and **V(C6)**, respectively, in the case of **TS-A**. The contribution of the basin populations arising from the butadiene and dienophile fragments to the variance of the population in the **V(C1,C6)** are ∼39% and ∼54%, respectively. This gives us a picture of fluctuation where the direction toward the butadiene fragment is favored around 15%. By considering then a simple balance between the electron populations in the basins associated with both the fragments and the corresponding positive nuclear charges, the charge separation at the **TS1-D** structure leaves an accumulation of charge on the butadiene fragment of 1.1e. The ELF picture of bonding provides further evidence that the ER dienophile **6** effectively behaves as a nucleophilic species toward the ED diene **1**.

In the case of **TS-A**, the net contribution to the fluctuation of **V(C1)** arising from the butadiene fragment accounts for ∼60%, whereas those arising from the dienophile fragment reach to ∼34% (including the contribution of the basin **V(C(6)**). On the opposite side, the net contribution to the fluctuation of **V-(C6)** coming from the dienophile and butadiene fragments are ∼55% and ∼34% (including the contribution of the basin **V-(C1)**), respectively. Considering the mutual contributions between **V(C1)** and **V(C6)** gives us a picture of electron delocalization favoring the direction from **V(C1)** toward **V(C6)** by ∼5%. This picture can be nicely associated to the observation of a net charge separation of 0.57e at the **TS-A** structure. The topologically based population analysis on both fragments reveals that such CT occurs from the ED diene **1** toward the ED dienophile **7**, as observed above from the NBO results. Despite the difference observed in the estimation of the CT values from the two methods, it is interesting to note that the favored **TS1-D** is predicted to be twice more polar than **TS-A**, both from the topological analysis of ELF and from that of the NBO results. Figure 3a,b represents the topology at different localization values of ELF domains for **TS1-D** and **TS-A**, respectively. We must emphasize in this point that these pictures do not represent the evolution of the charge transferring. By examining different decreasing values of the η isosurface, the shape of the electron delocalization in the region of the new bond forming C1−C6 can be clearly appreciated. In the case of **TS1-D**, at low localization values ($\eta = 0.65$), the monosynaptic basins associated with C2 are strongly delocalized on the **V(C1,C2)**, **V(C2,C7)**, and **V(C2,C3)** basins, as it can be interpreted from the contributions to the fluctuation of these population basins which accounts to ∼22% for each one.

In the region associated with the C1−C6 bond formation at **TS1-D**, it is clear that the **V(C1,C6)** basin indeed merges to the **V(C1,C2)** and the **V(C5,C6)** basins. This picture of delocalization can be associated with the above-described charge separation, which is delocalized from the **V(C5,C6)** basin in the ER dienophile **6** toward the **V(C1,C2)** basin of the diene **1**. The separation of each localization domain can be observed of course at higher values of η. Basin populations associated with the C1−C2, C2−C3, C3−C4, and C5−C6 bonding regions in the reactants (e.g., from independent ELF analyisis of **1** + **6**) are 3.46e, 2.13e, 3.46e, and 3.72e. In the **Zw** intermediate, the same populations become 2.10e, 2.50e, 3.46e, and 2.57e, where the new C1−C6 bonding region integrates only to 1.51e. Therefore, according to the formation of the endothermic intermediate **Zw**, formation of the **V(C1,C6)** basin at **TS1-D** can be seen as a manifestation of Hammond postulate.[31] On the other hand, Figure 3b reveals for **TS-A** that electron delocalization in the basins associated to the C1−C6 bond formation (e.g., **V(C1)** and **V(C6)**) exhibits a strong intercorrelation for $\eta < 0.72$. The delocalization is extended over the **V(C1,C2)** and the **V(C5,C6)** basins (e.g., see $\eta = 0.68$). It is clear that the formation of the C1−C6 bond in this case results from merging the **V(C1)** and **V(C6)** basins, in contrast to **TS1-D** for which, being the formation of the C1−C6 bond more advanced, the associated basin is indeed disynaptic. Likewise, the picture of delocalization for **TS-A** can be associated with the above-discussed charge separation, showing that it extends from the **V(C1,C2)** region in diene **1** toward the **V(C5,C6)** basin in the ED dienophile **7**.

These monosynaptic basins associated with C2 in **TS1-D** localizes 0.51e and 0.16e, and the populations located in the remaining disynaptic basins in the cyclic center of reaction **V-(C1,C2)**, **V(C2,C3)**, **V(C3,C4)**, and **V(C5,C6)** are respectively 2.42e (2.71 e), 2.34e (2.51e), 3.50e (3.19e), and 2.86e (3.07e) for **TS1-D** (**TS-A**). The **TS1-D** is certainly more advanced and more asynchronous than **TS-A**. We must note at this point that the basin population associated with the C5−C6 bonding region in reactants **6** and **7** are 2.84e and, as mentioned above, 3.72e. These basin populations give us a picture of bonding that is consistent with the above-discussed NBO results for these polar DA transition states. Note for instance that the charge depletion at C3−C4 in **TS-A** is more pronounced than those in **TS1-D**. The C2−C3 and C1−C2 populations become higher, in agreement with the above predicted CT direction toward the dienophile. The C5−C6 basin population is also less depleted in **TS-A** than in **TS1-D** showing that the charge is delocalized over the two CN groups (in about ∼6%).

It has also to be mentioned that the arrangement around C2 in **TS1-D** is AX3E2 like (see Figure 2) and that the disynaptic populations associated with the COOMe substitution at C2 and C3 are 2.55e (2.32) for **V(C2,C7)**, and 2.21e (2.27) for **V(C3,C8)**, respectively for **TS1-D (TS-A)**. This larger charge accumulation at the C2−C7 bond region in **TS1-D** is consistent with a picture of electron transferring from the dienophile to the diene, confirming that the COOMe group at the C2 position effectively delocalizes more electrons than that at the C3 one and that such an effect is more pronounced in **TS1-D** as compared with **TS-A**. The topological analysis of ELF complements the NBO picture of bonding, by indicating the shape of electron delocalization implied along the charge rearrangement in these polar DA reactions. The two methodologies consistently support that 2,3-dimethylenesuccinate **1** behaves as a nucleophile against the 1,1-dicyanoethylene **7** and as an electrophile when reacting with 2-methylene-1,3-dioxolane **6**.

In summary, the geometry parameters analysis and the electronic structure of the TSs allow us to establish that, at the polar DA reactions between ED 2,3-disusbtituted 1,3-butadienes as **1** and strong electrophilically activated dienophiles, only the C1−C2 π bond of the 1,3-butadiene mainly participates in the C−C bond formations at the first stage of the cycloaddition through highly asynchronous TSs. The second C3−C4 π bond of the diene can be seen as an electron-releasing substituent that stabilizes the positive charge that is being developed on the C2 carbon atom along the nucleophilic attack. As a consequence, the C3−C4 π bond cannot be involved in the formation of the second C−C σ bond at this stage of the reaction. (see Scheme 3).

4. Analysis of the Global Electrophilicity Index at the Ground State of the Reagents. Recent studies carried out on polar DA reactions[6] have shown that the indexes of reactivity defined within the conceptual DFT[11] are powerful tools to establish the polar character of the reactions. In Table 2, the static global properties, electronic chemical potential, μ, chemi-

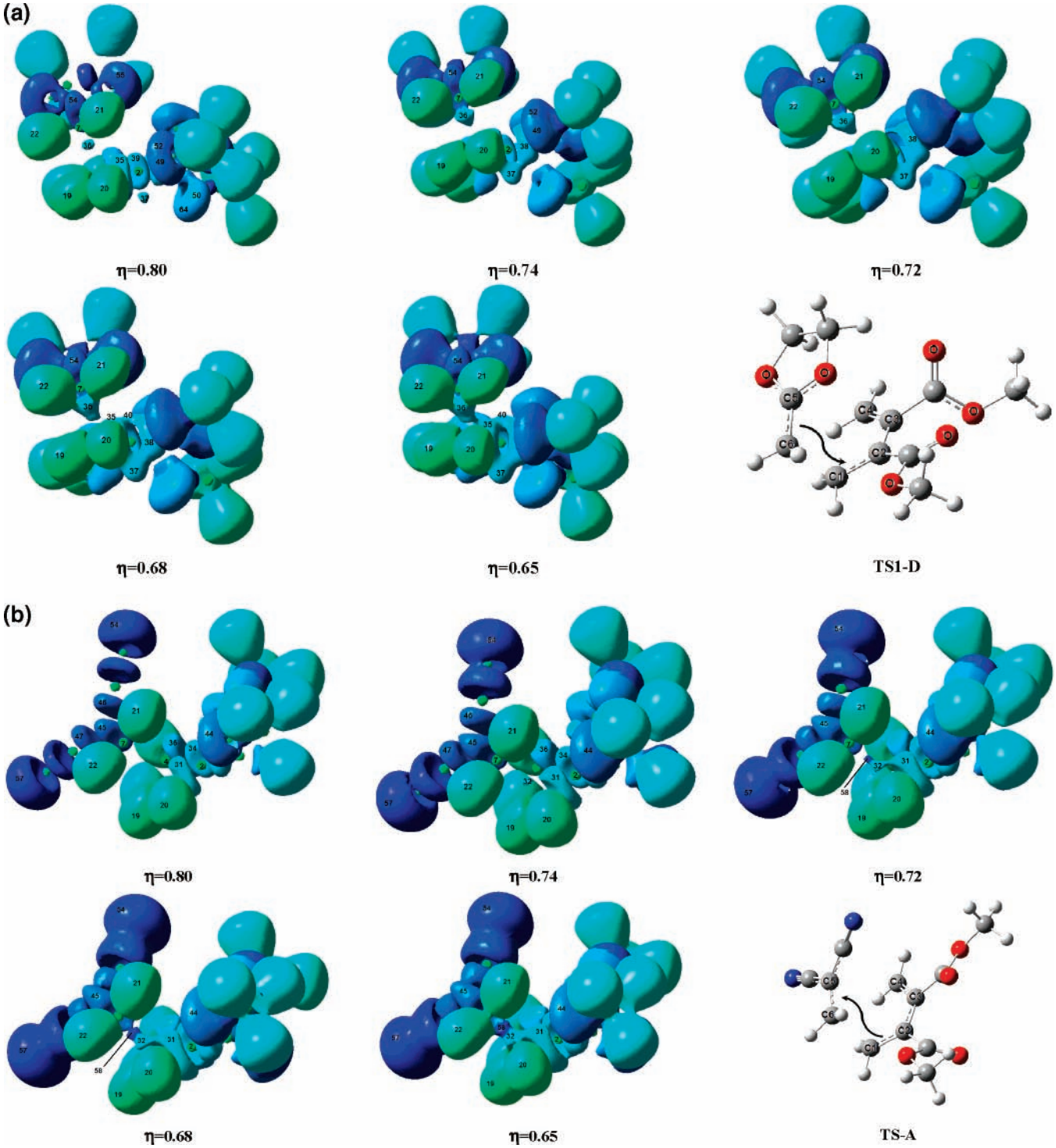

Figure 3. ELF isosurface pictures for different $\eta(\mathbf{r})$ values for (a) **TS1-D** and (b) **TS-A**. See the text for details.

cal hardness, η, and global electrophilicity, ω, for the 2,3-disubstituted diene **1** and the 1,1-disubstituted ethylenes **2**, **5**, **6**, and **7** are presented. It should be noted that, although the chemical potential allows us to establish the directionality of the charge transferring, it is the electrophilicity index that also incorporates the resistance to the electron charge to be deformed (e.g., hardness). The ω index has shown to be a key quantity allowing us the characterization of most important reagents used in cycloaddition reactions as strong, moderate, or marginal electrophiles within a unique scale.[6] In this context, it is just the difference in the electrophilicity index between dienes and dipolarophiles that has been postulated to be an indicator of the polarity of a DA reaction mechanism.[6]

The electronic chemical potentials of the ER ethylenes **2** and **6**, −0.0712 and −0.0724 au, respectively, are higher than that for the ED diene **1**, $\mu = -0.1560$ au. Therefore, along a polar interaction, the net CT will take place from these ER ethylenes toward the ED diene **1**, in clear agreement with the observed CT at **TS1-D**. On the other hand, the electronic chemical potential of the diene **1** is higher than those for the ED ethylenes **5** and **7**, −0.1683 and −0.2074 au, respectively. As a consequence, along a polar DA reaction, it is expected that the CT

SCHEME 3: Dual Electrophilic/Nucleophilic Behavior of the 1,2 Double Bond of the Diene 1 Where the Arrows Indicate the Fluctuation of the Charge Transfer at These Polar DA Reactions

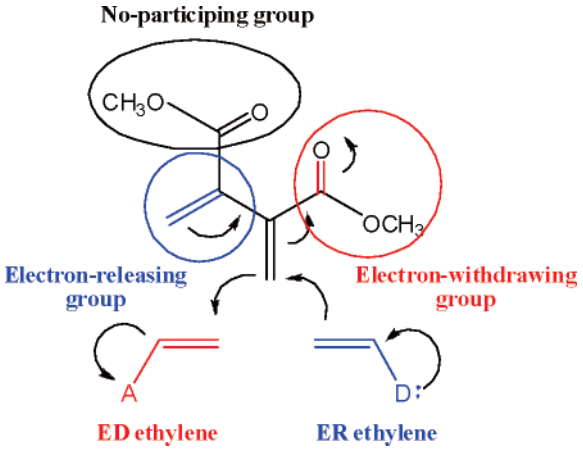

TABLE 2: Electronic Chemical Potential, μ in au, Chemical Hardness, η in au, and Global Electrophilicity, ω in eV, for the Dienes 1 and 10, and the ER Ethylenes 2 and 6, and the ED Ethylenes 5 and 7

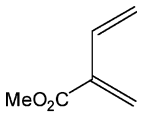

10

	μ	η	ω
7	−0.2074	0.2075	2.82
5	−0.1683	0.2135	1.80
10	−0.1478	0.1869	1.59
1	−0.1560	0.2099	1.58
11	−0.1288	0.1972	1.14
6	−0.0724	0.2674	0.27
2	−0.0712	0.2682	0.26

will take place from the diene **1** toward the ED ethylenes **5** and **7**, in clear agreement with the inversion of the flux of the observed CT at **TS-A**.

The electrophilicity of the ED diene **1** is 1.58 eV, a value that falls into the range of strong electrophiles within the ω scale.[6] The electrophilicity of methyl 2-methylenebut-3-enoate **10**, an ED 2-substituted 1,3-butadiene, is 1.59 eV. This value is similar to that for the ED diene **1**. The inclusion of one electron-withdrawing COOMe group on the C2 position on the butadiene system increases the electrophilicity of 1,3-butadiene **11** in 0. 45 eV. However, the inclusion of a second electron-withdrawing group on the C3 position has no appreciable effect on the electrophilicity value. These results are in agreement with those obtained from the geometrical and electronic analysis of **TS1-D** and **TS-A** in which the COOMe group on the C3 position of the butadiene has no appreciable role along these polar DA reactions. Consequently, it is expected that the analysis performed for the characterization of the nucleophilic behavior of these 2,3-disubstituted butadienes should be similar to that performed at 2-substituted butadienes as **10**.

The 1,1-disubstituted ethylenes **2** and **6** present very low electrophilicity values, 0.26 and 0.27 eV, respectively. They are classified as marginal electrophiles (good nucleophiles) within the ω scale.[6] Therefore, the DA reaction between the ED diene **1** and the ER ethyelenes **2** and **6**, which present a large $\Delta\omega$ value, 1.32 eV, will have a large polar character, in clear agreement with the large CT found at **TS1-D**. In these cases, the CT will take place from the ER ethylenes, acting as nucleophiles toward the ED diene **1** that acts as a electrophile (see the directions of the arrows in the Scheme 3).

On the other hand, the 1,1-disubstituted ethylenes **5** and **7** present high electrophilicity values, 1.80 and 2.82 eV, respectively. The presence of the two electron-withdrawing COOMe groups on the C1 position of the ethylene produces a larger electrophilic activation that the symmetric 2,3-disubstitucion on the diene **1**.[4c] On the other hand, the substitution of the two COOMe groups on **5** by two more electron-withdrawing CN groups increases the electrophilicity of **7**.[32] Note that, in the case of the cyanoethylene series, the inclusion of a second cyano group on ethylene increases notably the electrophilicity of **7**; $\Delta\omega$ = 1.10 eV relative to that for acrylonitrile.[4b]

These ED ethylenes present larger electrophilicity values than the diene **1**. Therefore, along a polar DA reaction, these ED ethylenes force the diene **1**, which is located below **5** and **7** in the electrophilicity scale, to behave as a nucleophile,[4c] allowing us to explain the inversion of the CT in these polar DA reactions (see the directions of the arrows in Scheme 3).

Therefore, it is expected that the ED dienes **1** and **10**, which are classified as a strong electrophile within the ω scale, will act as electrophiles toward ER ethylenes as **2** and **6** in polar DA reactions. This class of DA reactions has been classified as IED cycloadditions. However, these ED dienes can also act through its 1,3-butadiene system as nucleophiles toward strong activated ethylenes as **5** and **7** in polar DA reactions, which are classified as NED cycloadditions.

Finally, it is worth to remark that the electrophilic/nucleophilic behavior of these ED dienes can be better predicted by an analysis of reactivity indexes defined within the conceptual DFT than by the sole analysis based on the FMO framework because the reactions between ED reagents have closer HOMO−LUMO energy gaps. Finally, note that the IED or the NED character of the DA reactions is easily stabilized by looking at the relative positions of the diene and dienophile within the general electrophilicity scale.[6]

Conclusions

The electronic nature of the polar DA reactions of the ED dimethyl 2,3-dimethylenesuccinate **1** toward the nucleophilically activated dienophile **6** and the strong electrophilically activated dienophile **7** has been characterized by the NBO and ELF analysis of the electronic structure of the TSs involved in these cycloadditions using DFT methods at the B3LYP/6-31G(d) level. These TSs present a large zwitterionic character. For the polar DA reaction between the ED diene **1** and the strong electrophilically activated ethylene **7**, the charge-transfer flows from of diene **1**, which acts as nucleophile, toward the ethylene **7**. This behavior is clearly anticipated by an analysis of the electronic chemical potential and the electrophilicity power of the reagents.

Some relevant conclusions can be redrawn from the present study. At the highly asynchronous TSs associated with the first stage these polar DA reactions, the C−C bond-formation processes can be associated with a [2π (diene) + 2π (ethylene)] interaction instead of a [4π(diene) + 2π(ethylene)] interaction, more typical of a concerted process. From a molecular point of view, they are related to two- or four-center interaction reactions, respectively. As a consequence, at the first stage of the cycloaddition, only the C1−C2 double bond of the diene participates directly in the C−C bond formation. In the case of the DA reactions of the ED diene **1** toward ER ethylenes as **6**, the electron-withdrawing COOMe group is present on the C2

position of the diene that participates on the polar bond-formation process. However, toward strong electrophilically ethylenes as **7** is the C3−C4 double bond which participates in the C−C bond formation as an electron-releasing susbtituent. This participation allows a stabilization of the positive charge that is developing at the C2 carbon atom when the C1−C2 double bond of the diene behaves as a nucleophile. At this stage of the cycloaddition, the C3−C4 double bond does not participate on the formation of the second C−C σ bond as it occurs in the concerted [4π(diene) + 2π(ethylene)] cycloadditions. These behaviors, which are displayed in Scheme 3, allow us an explanation for the dual electrophilic/nucleophilic behavior of the 2-substituted and 2,3-disubstituted electron-deficient dienes as **10** and **1** in polar DA reactions.

Acknowledgment. This work was supported by research funds provided by the Ministerio de Educación y Ciencia of the Spanish Government (Project No. CTQ2006-14297/BQU) and the Generalitat Valenciana (GVACOMP/2007/082), and by Fondecyt Projects No. 1060961 (P.P.) and 1070378 (E.Ch.). E.Ch. and P.P. also thank the Universidad Andrés Bello (UNAB) by support through Project Nos. DI 21-06/R and 45-08/R, respectively. P.P. acknowledges the Generalidad Valenciana (AINV/2007/016). L.R.D. also thanks the Fondecyt Grant 7070051 for financial support. We finally gratefully acknowledge the Millennium Nucleus for Applied Quantum Mechanics and Computational Chemistry, P02-004-F (Conicyt-Mideplan) for continuous support.

Supporting Information Available: Complete information on the topological analysis of **TS1-D** and **TS-A** including basin populations, N_i, variance σ_i^2, relative fluctuation λ_i, and main contributions arising from other basins j(%) to the fluctuation (σ_i^2) of basin population i, for **TS1-D** and **TS-A**, respectively. This material is available free of charge via the Internet at http://pubs.acs.org.

References and Notes

(1) (a) Carruthers, W. *Some Modern Methods of Organic Synthesis*; second ed.; Cambridge University Press: Cambridge, 1978. (b) Carruthers, W. *Cycloaddition Reactions in Organic Synthesis*; Pergamon: Oxford, 1990.

(2) (a) Diels, O.; Alder, K. *Justus Liebigs Ann. Chem.* **1928**, *460*, 98. (b) Woodward, R. B.; Hoffmann, R. *Angew. Chem., Int. Ed. Engl.* **1969**, *8*, 781.

(3) (a) Sustmann, R.; Sicking, W. *J. Am. Chem. Soc.* **1996**, *118*, 12562. (b) Sustmann, R.; Tappanchai, S.; Bandmann, H. *J. Am. Chem. Soc* **1996**, *118*, 12555.

(4) (a) Domingo, L. R.; Arnó, M.; Andrés, J. *J. Org. Chem.* **1999**, *64*, 5867. (b) Domingo, L. R.; Aurell, M. J.; Pérez, P.; Contreras, R. *J. Org. Chem.* **2003**, *68*, 3884. (c) Domingo, L. R. *Eur. J. Org. Chem.* **2004**, 4788.

(5) Parr, R. G.; von Szentpaly, L.; Liu, S. *J. Am. Chem. Soc.* **1999**, *121*, 1922.

(6) (a) Domingo, L. R.; Aurell, M. J.; Pérez, P.; Contreras, R. *Tetrahedron* **2002**, *58*, 4417. (b) Pérez, P.; Domingo, L. R.; Aizman, A.; Contreras, R. In *Theoretical Aspects of Chemical Reactivity*; Toro-Labbé, A., Ed.; Elsevier Science: New York, 2006; Vol. 19, p 167.

(7) Spino, C.; Rezaei, H.; Dory, Y. L. *J. Org. Chem.* **2004**, *69*, 757.

(8) (a) Fukui, K. *Molecular Orbitals in Chemistry, Physics, and Biology*; Academic: New York, 1964. (b) Fukui, K. *Acc. Chem. Res.* **1971**, *4*, 57. (c) Fukui, K. *Acc. Chem. Res.* **1981**, 363.

(9) (a) Phino e Melo, T. M. V. D.; Fausto, R.; Rocha Gonsalves, A. M. d. A.; Gilchrist, T. L. *J. Org. Chem.* **1998**, 5350. (b) Sisti, N. J.; Motorina, I. A.; Tran Huu Dau, M.-E.; Riche, C.; Fowler, F. W.; Grierson, D. S. *J. Org. Chem.* **1996**, *61*, 3715.

(10) (a) McIntosh, J. M.; Sieler, R. A. *J. Org. Chem.* **1978**, *43*, 4431. (b) Spino, C.; Crawford, J. *Can. J. Chem.* **1993**, *71*, 1094. (c) Spino, C.; Crawford, J.; Gugelchuk, M.; Cui, Y. *J. Chem. Soc., Perkin Trans. 2* **1998**, 1499.

(11) (a) Geerlings, P.; De Proft, F.; Langenaeker, W. *Chem. Rev.* **2003**, *103*, 1793. (b) Ess, D. H.; Jones, G. O.; Houk, K. N. *Adv. Synth. Catal.* **2006**, *348*, 2337.

(12) (a) Becke, A. D. *J. Chem. Phys.* **1993**, *98*, 5648. (b) Lee, C.; Yang, W.; Parr, R. G. *Phys. Rev. B* **1988**, *37*, 785.

(13) Hehre, W. J.; Radom, L.; Schleyer, P. v. R.; Pople, J. A. *Ab initio Molecular Orbital Theory*; Wiley: New York, 1986.

(14) (a) Schlegel, H. B. *J. Comput. Chem.* **1982**, *3*, 214. (b) Schlegel, H. B. *Geometry Optimization on Potential Energy Surface. In Modern Electronic Structure Theory*; Yarkony, D. R., Ed.; World Scientific Publishing: Singapore, 1994.

(15) Fukui, K. *J. Phys. Chem.* **1970**, *74*, 4161.

(16) (a) González, C.; Schlegel, H. B. *J. Phys. Chem.* **1990**, *94*, 5523. (b) González, C.; Schlegel, H. B. *J. Chem. Phys.* **1991**, *95*, 5853.

(17) (a) Reed, A. E.; Weinstock, R. B.; Weinhold, F. *J. Chem. Phys.* **1985**, *83*, 735. (b) Reed, A. E.; Curtiss, L. A.; Weinhold, F. *Chem. Rev.* **1988**, *88*, 899.

(18) Becke, A. D.; Edgecombe, K. E. *J. Chem. Phys.* **1990**, *92*, 5397.

(19) (a) Savin, A.; Becke, A. D.; Flad, J.; Nesper, R.; Preuss, H.; Vonschnering, H. G. *Angew. Chem., Int. Ed. Engl.* **1991**, *30*, 409. (b) Savin, A.; Nesper, R.; Wengert, S.; Fassler, T. F. *Angew. Chem., Int. Ed. Engl.* **1997**, *36*, 1809. (c) Silvi, B. *J. Mol. Struct.* **2002**, *614*, 3. (d) Savin, A.; Silvi, B.; Colonna, F. *Can. J. Chem.* **1996**, *74*, 1088. (e) Silvi, B.; Savin, A. *Nature* **1994**, *371*, 683. (f) Silvi, B. *Phys. Chem. Phys.* **2004**, *6*, 256. (g) Ponec, R.; Chaves, J. *J. Comput. Chem.* **2005**, *26*, 1205. (h) Matito, E.; Silvi, B.; Duran, M.; Sola, M. *J. Chem. Phys.* **2006**, *125*, 024301.

(20) (a) Chamorro, E.; Notario, R.; Santos, J. C.; Pérez, P. *Chem. Phys. Lett.* **2007**, *443*, 136. (b) Cárdenas, C.; Chamorro, E.; Notario, R. *J. Phys. Chem. A* **2005**, *109*, 4352. (c) Chamorro, E.; Notario, R. *J. Chem. Phys. B* **2005**, *109*, 7594. (d) Chamorro, E.; Notario, R. *J. Chem. Phys. A* **2004**, *109*, 4099. (e) Chamorro, E. *J. Chem. Phys.* **2003**, *118*, 8687. (f) Chamorro, E.; Santos, J. C.; Gómez, B.; Contreras, R.; Fuentealba, P. *J. Phys. Chem. A* **2002**, 106, 11533. (g) Fuentealba, P.; Chamorro, E.; Santos, J. C. In *Theoretical Aspects of Chemical Reactivity*; Toro-Labbe, A., Ed.; Elsevier: Amsterdam, 2006; Vol. 19, p 57. (h) Silvi, B.; Fourré, I.; Alikhani, M. E. *Mon. F. Chem.* **2005**, *136*, 855. (i) Melin, J.; Fuentealba, P. *Inter. J. Quantum. Chem.* **2003**, *92*, 381. (j) Santos, J. C.; Tiznado, W.; Contreras, R.; Fuentealba, P. *J. Chem. Phys.* **2004**, *120*, 1670. (k) Santos, J. C.; Andrés, J.; Aizman, A.; Fuentealba, P. *J. Chem. Theor. Comput.* **2005**, *1*, 83.

(21) (a) Silvi, B. *Phys. Chem. Phys.* **2004**, *6*, 256. (b) Bader, R. F. W.; Stephens, M. E. *J. Am. Chem. Soc.* **1975**, *97*, 7391. (c) Fradera, X.; Austen, M. A.; Bader, R. F. W. *J. Phys. Chem. A* **1999**, *103*, 304. (d) Angyan, J. G.; Loos, M.; Mayer, I. *J. Phys. Chem.* **1994**, *98*, 5244. (e) Ponec, R.; Strnad, M. *Int. J. Quantum Chem.* **1994**, *50*, 43. (f) Ponec, R.; Uhlik, F. *J. Mol. Struct.* **1997**, *391*, 159.

(22) (a) Berski, S.; Andres, J.; Silvi, B.; Domingo, L. R. *J. Phys. Chem. A* **2003**, *107*, 6014. (b) Polo, V.; Domingo, L. R.; Andres, J. *J. Phys. Chem. A* **2005**, *109*, 10438. (c) Berski, S.; Andres, J.; Silvi, B.; Domingo, L. R. *J. Phys. Chem. A* **2006**, *110*, 13939. (d) Domingo, L. R.; Picher, M. T.; Arroyo, P.; Saez, J. A. *J. Org. Chem.* **2006**, *71*, 9319. (e) Polo, V.; Domingo, L. R.; Andres, J. *J. Org. Chem.* **2006**, *71*, 754.

(23) Noury, S.; Krokidis, X.; Fuster, F.; Silvi, B. *Comput. Chem.* **1999**, *23*, 597.

(24) Frisch, M. J.; Trucks, G. W.; Schlegel, H. B.; Scuseria, G. E.; Robb, M. A.; Cheeseman, J. R.; Montgomery, J., J. A.; Vreven, T.; Kudin, K. N.; Burant, J. C.; Millam, J. M.; Iyengar, S. S.; Tomasi, J.; Barone, V.; Mennucci, B.; Cossi, M.; Scalmani, G.; Rega, N.; Petersson, G. A.; Nakatsuji, H.; Hada, M.; Ehara, M.; Toyota, K.; Fukuda, R.; Hasegawa, J.; Ishida, M.; Nakajima, T.; Honda, Y.; Kitao, O.; Nakai, H.; Klene, M.; Li, X.; Knox, J. E.; Hratchian, H. P.; Cross, J. B.; Adamo, C.; Jaramillo, J.; Gomperts, R.; Stratmann, R. E.; Yazyev, O.; Austin, A. J.; Cammi, R.; Pomelli, C.; Ochterski, J. W.; Ayala, P. Y.; Morokuma, K.; Voth, G. A.; Salvador, P.; Dannenberg, J. J.; Zakrzewski, V. G.; Dapprich, S.; Daniels, A. D.; Strain, M. C.; Farkas, O.; Malick, D. K.; Rabuck, A. D.; Raghavachari, K.; Foresman, J. B.; Ortiz, J. V.; Cui, Q.; Baboul, A. G.; Clifford, S.; Cioslowski, J.; Stefanov, B. B.; Liu, G.; Liashenko, A.; Piskorz, P.; Komaromi, I.; Martin, R. L.; Fox, D. J.; Keith, T.; Al-Laham, M. A.; Peng, C. Y.; Nanayakkara, A.; Challacombe, M.; Gill, P. M. W.; Johnson, B.; Chen, W.; Wong, M. W.; Gonzalez, C.; Pople, J. A. *Gaussian 03*, Revision D.01; Gaussian, Inc.: Wallingford, CT, 2004.

(25) Chattaraj, P. K.; Sarkar, U.; Roy, D. R. *Chem. Rev.* **2006**, *106*, 2065.

(26) (a) Parr, R. G.; Yang, W. *Density Functional Theory of Atoms and Molecules*; Oxford University Press: New York, 1989. (b) Parr, R. G.; Pearson, R. G. *J. Am. Chem. Soc.* **1983**, *105*, 7512.

(27) Goldstein, E.; Beno, B.; Houk, K. N. *J. Am. Chem. Soc.* **1996**, *118*, 6036.

(28) Robiette, R.; Marchand-Brynaert, J.; Peeters, D. *J. Org. Chem.* **2002**, *67*, 6823.

(29) Dewar, M. J. S.; Olivella, S.; Stewart, J. J. P. *J. Am. Chem. Soc.* **1986**, *108*, 5771.

(30) Wiberg, K. B. *Tetrahedron* **1968**, *24*, 1083.

(31) Hammond, G. S. *J. Am. Chem. Soc.* **1955**, *77*, 334.

(32) Domingo, L. R.; Pérez, P.; Contreras, R. *J. Org. Chem.* **2003**, *68*, 6060.